Pricing Beyond Insurance:
Capital Markets and Emerging Risks

Marcel Freyschmidt*

The evolving risk landscape presents significant challenges for both private and public entities. Traditionally, risk sharing is straightforward, defined by the relationship between policyholders and insurance companies. However, emerging risks such as climate change and cyber threats, along with increasingly severe events, are now also being underwritten by the capital markets. In these cases, (re)insurers or brokers often hedge their risks through catastrophe or cyber bonds. Due to their uncorrelated nature with capital market risks, these alternative investment products offer attractive portfolio diversification opportunities and high returns, which traditional pricing and factor models cannot adequately explain. This study introduces a comprehensive pricing model that incorporates market conditions, correlation structures, and extreme jump risks. Applying this model to real-world data, including hurricane losses and cyber risks, demonstrates its relevance and accuracy in deriving market prices. By calibrating the model to market data, a unique probability distortion is identified through measure transformation, even in an incomplete market. This approach allows for a detailed comparison of the risk appetites of different entities and provides a sustainable understanding of these emerging markets.

Keywords: Emerging Risk, NatCat Risk, Cyber Risk, Cat Bond, Cyber Bond, Option Pricing, Jump Processes, Tail Risk

*marcel.freyschmidt@unisg.ch; Girtannerstrasse 6, CH-9010 St.Gallen; Phone +41 71 224 7974.

1 Introduction

The increasing frequency and severity of natural disasters driven by climate change have expanded the scope of private risk-sharing beyond traditional property and casualty risks. Additionally, the rise of cyber threats due to global networking and digitalization has further broadened this scope, challenging the conventional policyholder-insurer relationship. Insurance-linked securities, such as catastrophe bonds and cyber bonds, actively involve the capital markets in risk sharing today. In this system, (re)insurers or brokers initially underwrite these (tail) risks with the policyholder but subsequently transfer them to the capital markets. As a result, they function as policyholders themselves to secure protection from the capital markets in the event of a triggering event. These risks are largely uncorrelated with capital market risks, making them attractive for investment due to their high returns and diversification potential (Cummins and Weiss, 2009). However, severe losses, as exemplified by the Covid-19 pandemic, push the limits of the capital market and underscore the necessity for government involvement (e.g., Gründl et al., 2021; Braun et al., 2023).

With the rise of climate and cyber risks, along with the recent Covid-19 pandemic, the presence of jump risks and their correlation with macroeconomic fundamentals has become increasingly important. In financial markets, these factors are crucial in high-volatility areas like oil and electricity, and in hedging against stock market crashes (e.g., Caldana and Fusai, 2013). Consequently, research on tail risks and risk premiums in financial markets is extensive. Using S&P 500 data, Bollerslev and Todorov (2011) and Kelly and Jiang (2014) show that a significant portion of the observed risk premiums compensates for rare events. Andersen et al. (2020) demonstrate that compensation for negative jump risk is the primary driver of premiums in international options markets. In a more general context, Ai and Bhandari (2021) show that exposure to downside tail risk leads to quantitatively large and volatile risk premium. Understanding and replicating the returns of cat bond markets, where this risks are underwritten, is a relatively new area. Using traditional asset pricing models such as factor models or consumption-based models can only explain small parts of the risk premium (e.g., Braun et al., 2023). Empirical findings in the corporate bond literature also indicate that factor models cannot adequately describe the risk premium (Dickerson et al., 2023).

The pricing of extreme risks is based on three key principles (Zanjani, 2002): (1) shareholders may not be able to cover large, unexpected losses; (2) shareholders expect to be compensated for the risks they take; and (3) policyholders are concerned about the risk of the company becoming insolvent. Calibrating the second principle with real-world data is particularly challenging. The lack of high-frequency extreme risk data and models for calibrating frictions and risk premiums has led to the frequent use of unsuitable models in the literature, such as those by Fama and French (1993) for financial institutions (e.g., Cummins and Phillips, 2005). Factor models for the cat bond market also explain only a small part of the risk premium (e.g., Braun et al., 2019a). For other risks such as cyber or pandemic, there is a lack of long-term data, as the cyber bond market is relatively new, or the absence of established markets for certain risks, such as pandemics (e.g., Gründl et al., 2021). A model that consistently includes the market environment, correlation structures, and jump risks, while accounting for higher-order factors, is still missing.

Addressing this gap, this paper makes three key contributions. First, it assigns a stochastic framework to each of the four risk categories from Cummins (2006), aligning them with market conditions. This approach simplifies the process of determining necessary players, such as whether a risk should be transferred to the capital market. Second, the study introduces a comprehensive model for pricing the different risk categories and determining risk premiums, integrating it with established option models. Since options themselves are a hedging instrument for financial markets, this approach is particularly suitable for pricing capital market products such as cat bonds or cyber bonds. The model deviates from traditional insurance approaches by considering the market environment, correlation structures, and jump risks, while accounting for higher-order factors, and maintains a consistent framework for all risk categories. Grounded in the model proposed by Doherty and Garven (1986), it includes shareholders and policyholders and accounts for government frictions like taxes. Central to this analysis are models from Margrabe (1978), focusing on the exchange dynamics of two risky assets, and Merton (1976), incorporating jump risks. Additionally, the closed-form solution by Cheang and Chiarella (2011) integrates these models effectively. The underlying actuarial principle is the measure transformation as described by Esscher (1932), Gerber and Shiu (1994), and Wang (2000), which can be characterized as probability distortion. While the distortion is unique in simpler cases, it is not in the general case of an incomplete market. In economic terms, Gao et al. (2019) describe this distortion as tail risk concerns, which reflect investors' subjective ex-ante beliefs about tail risk. Third, the paper demonstrates the practical application of this new methodology using real loss estimates. By calibrating model parameters with market data, the paper prices cat bonds and cyber bonds. Despite friction and jump risk, precise market calibration allows for the calculation of a unique measure $\mathbb{Q}$ for individual markets or entities, enabling a comparison of the risk appetite across them, thus exceeding factor or consumption-based models. This paper provides initial evidence that, unlike the classic bond market, the spread in cat and cyber bonds primarily depends on investors' tail risk concerns, leading to a homogeneous and unique risk profile determined by $\mathbb{Q}$, independent of the cedent.

This paper is structured as follows. Section 2 introduces the model, defines its boundaries, and describes its connection to existing pricing models. Section 3 demonstrates the market application. Section 4 concludes.

2 Model

2.1 Risk categories

To determine which risks adhere to the traditional policyholder-(re)insurance framework and at what point capital market involvement or government backstops are required, it is essential to categorize them. This paper defines four risk categories based on the framework proposed by Cummins (2006) and assigns each a mathematical framework. It is important to note that these categories are not mutually exclusive. For instance, cyber risk may be managed through traditional (re)insurance, transferred to the capital markets, or involve discussions of government backstops, depending on the severity and quantile of the cumulative distribution function addressed (see, e.g., Kasper et al., 2024). The risk categories can be summarized as follows:

- *Locally Insurable:* Pertains to independent risks characterized by moderate standard deviations per risk and a substantial number of policies, such as the U.S. market for personal automobile insurance. Local insurers can effectively cover these losses.
- *Globally Insurable:* Encompasses risks that are locally dependent but globally independent, such as tornadoes in the American Midwest versus Australia. Local insurers may lack the capacity to cover such losses, but global reinsurers can. Consequently, these risks are diversifiable on a global scale through reinsurance.
- *Globally Diversifiable:* Refers to risks with low frequency and very high severity, such as a $100 billion event in Florida or California. The capacity of insurance and reinsurance companies may prove insufficient to cover such events, but these risks can be globally diversified through capital markets.
- *Globally Undiversifiable:* Describes risks of such severity that they may resist global diversification, even through capital markets. For instance, a severe earthquake in Tokyo with losses ranging from $2.1 to $3.3 trillion. While global securities markets might absorb a fraction of such a loss, complete diversification of the full loss is unlikely, and government aid is likely needed.

Despite the economic coherence and comprehensiveness of these categories, which encompass all relevant private and public risk bearers, it is essential to address the underlying mathematical nuances. Cummins falls short in today's market environment, particularly for the last two categories.[1]

Local insurable risks follow a straightforward framework based on the law of large numbers, assuming independence of losses within a loss portfolio. However, this independence does not apply when examining globally insurable risks from a local perspective. On a global scale, these risks exhibit no interdependence, allowing the creation of a loss portfolio of independent losses. Thus, while there may be variations in the sizes of loss portfolios, local and global insurable risks are mathematically comparable and can be modeled using right-skewed and independent random variables (e.g., Eling, 2012). Globally diversifiable and globally undiversifiable risks share characteristics of low frequency and high severity, with heavy tail events significantly influencing these risk profiles. They follow a structure of jump processes, such as a compounded Poisson process (e.g., Merton, 1976; Lee and Yu, 2002), which is a common assumption of the actuarial literature (e.g., Bowers et al., 1986). A key distinction lies in the severity of globally undiversifiable risks, which can directly impact macroeconomic fundamentals. These risks uniquely correlate with the economy and can trigger worldwide shocks, as seen with the Covid-19 pandemic (e.g., Gründl et al., 2021; Braun et al., 2023). Mathematically, in the first case, the occurrence of jumps and the jump size are uncorrelated, while in the latter case, there is a joint jump process with correlated jump sizes.

[1] Cummins defines the last two categories of catastrophes as events that violate the principal insurability condition and may be globally diversifiable through capital markets if other conditions are satisfied. He does not specify mathematical concepts for these categories, unlike the first two.

2.2 Shareholder and Policyholder

Inspired by Doherty and Garven (1986), a single-period model is considered. In $t = 0$ shareholders contribute equity S_0 and policyholders pay premiums P to cover the stochastic loss $\bar{L}$. The shareholder's opening cash flow is:

$$Y_0 = S_0 + P,$$

where the cash flow is invested at a risky rate $\bar{r}$. The terminal cash flow is:[2]

$$\bar{Y}_1 = (1 + \bar{r})\big(S_0 + P\big).$$

At the end of the period, the policyholders claim $\bar{L} \geq 0$, and the government (or other organizations such as supervisory authorities) claims frictional costs like monitoring, agency or taxes $\bar{T}_1 \geq 0$. The policyholders receive the payment:

$$\begin{aligned} \bar{H}_1 &= min(\bar{L}, \bar{Y}_1) \\ &= \bar{Y}_1 - max(\bar{Y}_1 - \bar{L}, 0), \end{aligned}$$

and the additional frictional costs are:

$$\bar{T}_1 = max[\tau(\bar{Y}_1 - \bar{L}), 0],$$

where τ is the rate for frictional costs.[3]

Both claims exhibit cash flows analogous to a European call option,[4] so the present values are:

$$\begin{aligned} H_0 &= V(\bar{Y}_1) - C(\bar{Y}_1; \bar{L}) \\ T_0 &= \tau C(\bar{Y}_1; \bar{L}), \end{aligned}$$

where $V(\cdot)$ is a present valuation operator and $C(A; B)$ is the current market value of a European call option with a terminal value A and exercise price B.

The present market value of the shareholder's return on equity, V_e, is the difference between the market value of the portfolio, $V(\bar{Y}_1)$, on the one side, and the present value of the policyholders' claims and the present value of the frictional costs on the other side:

$$\begin{aligned} V_e &= V(\bar{Y}_1) - H_0 - T_0 \\ &= C(\bar{Y}_1; \bar{L}) - \tau C(\bar{Y}_1; \bar{L}). \end{aligned}$$

[2] Doherty and Garven (1986) incorporate an adjustment to the premium investment by applying a coefficient for fundraising. This adjustment compensates for the temporal misalignment between the model period and the average delay between premium receipt and claims payment. For the sake of model simplicity, this adjustment is not included here.

[3] In the context of Doherty and Garven (1986), τ signifies the corporate tax rate, exclusively applied to income. Thus, $\bar{T}_1 = \max[\tau(\bar{Y}_1 - Y_0 + P - \bar{L}), 0]$. However, this depiction is excessively limiting, especially concerning capital market involvement and overall capital costs in the context of jump risk, as discussed in Zanjani (2002). Therefore, this aspect is further expounded upon here.

[4] The cash flow of a European call option is $CF_{call} = max(A - B, 0)$ with terminal value A and exercise price B.

In summary, shareholders hold a long position in a call option on the pre-frictional terminal value of the asset portfolio and a short position in a call option on the frictions of that portfolio.

Risk transfer prices are determined to yield a fair return to shareholders, achieved when the current market value of the equity claim equals the initial investment. As $\bar{Y}_1$ and Y_0 are functions contingent on P, the objective is to identify the premium P^* that satisfies:

$$\begin{aligned} V_e &= C(\bar{Y}_1(P^*); \bar{L}) - \tau C(\bar{Y}_1(P^*); \bar{L}) \\ &= S_0. \end{aligned} \tag{OM}$$

Calculating P^* necessitates employing a suitable option-pricing framework. While Doherty and Garven (1986) establish pricing relationships within the discrete-time, risk-neutral-valuation framework of Rubinstein (1976), focusing on two special cases with (log-) normally distributed stochastic components[5], this study extends the analysis to stochastic processes and accounting for jump risks. Given the stochastic nature of the exercise price, conventional models like Black and Scholes (1973) are impractical. In a globally expanding world with increased climate and cyber risks, the emphasis on global diversification, including capital markets, and consideration of tail risks is becoming increasingly important.

2.3 Pricing the option

Consider tradable assets X_1 and X_2 under a probability measure $\mathbb{P}$. Extending the option price formula from Black and Scholes (1973), Margrabe (1978) formulated a model allowing the exchange of two risky assets. It is assumed that all returns come from capital gains and that no dividends are distributed.[6] The dynamics for each asset are expressed as:

$$\frac{dX_i}{X_i} = \mu_i dt + \sigma_i dW_{i,t} \qquad i \in \{1, 2\},$$

where μ_i is the instantaneous expected return per unit time, σ_i is the instantaneous volatility per unit time and both assets follow a Brownian motion $dW_{i,t}$ with correlation ρ. This setting has the closed-form solution:

$$\begin{aligned} C(X_1, X_2) &= X_1 \Phi(d_1) - X_2 \Phi(d_2) \\ \text{with} \quad d_1 &= \frac{ln(\frac{X_1}{X_2}) + \frac{1}{2}\sigma^2 (T-t)}{\sigma\sqrt{T-t}} \\ d_2 &= d_1 - \sigma\sqrt{T-t}. \end{aligned}$$

$T - t$ represents the difference between the exercise period and the present period, $\Phi(\cdot)$ is the cumulative standard normal density function, and $\sigma^2 = \sigma_1^2 - 2\sigma_1\sigma_2\rho + \sigma_2^2$.[7]

[5]Distribution assumptions like the normal distribution prove inadequate, as highlighted by Eling (2012).

[6]The examination of dividend payout, as discussed in papers such as Cheang and Chiarella (2011), can be easily incorporated into the model. However, since it does not constitute a central core here, it is omitted to prevent additional complexity, but discussed in Appendix A.2.

[7]For $\sigma^2 = \sigma_1^2$ and $\sigma_2 = 0$, the formula from Black and Scholes (1973) is obtained.

Globally diversifiable and globally undiversifiable risks are characterized by low frequency and high-severity events that fall beyond the scope of Margrabe (1978). The emergence of globally undiversifiable risk is inherently tied to economic fundamentals, indicating that not only does the loss portfolio but also the asset side exhibit a correlated downside risk. Modeling tail risk involves incorporating jump processes, aligning with the conceptual framework established in Merton (1976). Unlike Margrabe, Merton's model does not consider the exchange of two risky assets but follows the methodology of Black and Scholes (1973). Consequently, a synthesis of both approaches becomes essential in this context.

Let N_t be a Poisson process with a constant arrival rate of jumps λ, shared by both stocks. The bivariate process $\boldsymbol{Y} = (Y_1, Y_2)^T$ represents the jump sizes, taking values $\boldsymbol{y} = (y_1, y_2)^T \in \mathbb{R}^2$. The jump sizes Y_n are independently and identically distributed as multivariate normal $\mathcal{N}(\boldsymbol{\alpha}, \Sigma_{\boldsymbol{Y}})$, where $\boldsymbol{\alpha} = (\alpha_1, \alpha_2)^T$, and the covariance matrix $\Sigma_{\boldsymbol{Y}}$ is given by:

$$\Sigma_{\boldsymbol{Y}} = \begin{pmatrix} \delta_1^2 & \rho_{\boldsymbol{Y}}\delta_1\delta_2 \\ \rho_{\boldsymbol{Y}}\delta_1\delta_2 & \delta_2^2 \end{pmatrix}$$

with $\rho_{\boldsymbol{Y}}$ representing the correlation between the jump sizes Y_1 and Y_2. The expected proportional common jump sizes are expressed as:

$$\kappa_i = \mathbb{E}_{\mathbb{P}}[\exp(Y_i) - 1)] = \int_{\mathbb{R}} [\exp(Y_i) - 1] m_{\mathbb{P}}(dy_i) \qquad i \in \{1, 2\},$$

where $m_{\mathbb{P}}(dy_i)$ is the density of Y_i (e.g., Merton, 1976).

Next, let $N_{i,t}$ be a Poisson process with a constant arrival rate of jumps λ_i and jump size Z_i, taking values $z_i \in \mathbb{R}$ for $i \in \{1, 2\}$. These processes are uncorrelated and specific to each asset. The idiosyncratic jump sizes are independently and identically normal-distributed as $\mathcal{N}(\alpha_{ii}, \delta_{ii}^2)$. The expected proportional unique jump sizes are given by:

$$\kappa_{Z_i} = \mathbb{E}_{\mathbb{P}}[\exp(Z_i) - 1] = \int_{\mathbb{R}} [\exp(Z_i) - 1] m_{\mathbb{P}}(dz_i) \qquad i \in \{1, 2\},$$

where $m_{\mathbb{P}}(dz_i)$ is the density of Z_i.

In summary, for each asset, the n-th common jumps $Y_{1,n}$ and $Y_{2,n}$ occur simultaneously, determined by the same Poisson arrival process N_t. These jointly occurring jumps can be linked to macroeconomic shocks in the system, representing globally undiversifiable risks. On the other hand, the m-th jump $Z_{1,m}$ or k-th jump $Z_{2,k}$, specific to the i-th asset, is determined by the Poisson arrival process $N_{i,t}$. Jumps unique to each stock can be attributed solely to idiosyncratic shocks for that particular asset, defining globally diversifiable risks.

The return dynamics of the assets can be expressed as:

$$\begin{aligned} \frac{dX_i}{X_i} =& (\mu_i - \lambda\kappa_i - \lambda_i\kappa_{Z_i})dt + \sigma_i dW_{i,t} \\ &+ \int_{\mathbb{R}} [\exp(y_i) - 1] p(dy_i, dt) + \int_{\mathbb{R}} [\exp(z_i) - 1] p(dz_i, dt) \qquad i \in \{1, 2\}, \end{aligned}$$

where $p(\cdot, dt)$ is the Poisson measure. Poisson measures and the bivariate Wiener process are independent. The stock prices are given by the solution:

$$S_{i,t} = S_{i,0} \exp\left(\left(\mu_i - \lambda\kappa_i - \lambda_i \kappa_{Z_i} - \frac{\sigma_i^2}{2}\right)t + \sigma W_{i,t} + \sum_{n=1}^{N_t} Y_{i,n} + \sum_{m=1}^{N_{i,t}} Z_{i,m} \right) \qquad i \in \{1, 2\}.$$

To achieve a suitable and fair evaluation of the final payoff conditioned on information about the underlying asset prices, the probability measure $\mathbb{P}$ is transformed to $\mathbb{Q}$ using the transformation proposed by Esscher (1932), see Appendix A.1. After applying the transformation, the change in the intensity is defined by:

$$\begin{aligned}
\tilde{\lambda} &= \lambda \mathbb{E}_{\mathbb{P}}[\exp(\boldsymbol{\gamma}^T \boldsymbol{Y})] \\
\tilde{\lambda}_1 &= \lambda_1 \mathbb{E}_{\mathbb{P}}[\exp(\beta_1 Z_1)] \\
\tilde{\lambda}_2 &= \lambda_2 \mathbb{E}_{\mathbb{P}}[\exp(\beta_2 Z_2)],
\end{aligned}$$

and the expected jump sizes are transformed to:

$$\begin{aligned}
\tilde{\kappa}_i &= \mathbb{E}_{\mathbb{Q}}[\exp(Y_i) - 1] \qquad i \in \{1, 2\} \\
\tilde{\kappa}_{Z_i} &= \mathbb{E}_{\mathbb{Q}}[\exp(Z_i) - 1] \qquad i \in \{1, 2\}.
\end{aligned}$$

Hence, under $\mathbb{Q}$, the distribution of the jump sizes also changes. Y_n remains independently and identically multivariate normally distributed with $\tilde{\boldsymbol{\alpha}} = \boldsymbol{\alpha} + \Sigma_{\boldsymbol{Y}} \boldsymbol{\gamma}$; the jump sizes $Z_{i,k}$ are independently and identically normally distributed with $\tilde{\alpha}_{ii} = \alpha_{ii} + \delta_{ii}^2 \beta_i$ for $i \in \{1, 2\}$.

The parameters $\boldsymbol{\gamma}$ for the joint process, and β_i with $i \in \{1, 2\}$ for the distinct processes, are fundamental factors in the transition from $\mathbb{P}$ to $\mathbb{Q}$. The market, comprising stocks with jump components, is inherently incomplete following the sense of Harrison and Pliska (1981). When accounting for market prices of jump risks, multiple equivalent martingale measures emerge, leading to different option prices. For instance, if all factors equal zero, the scenario is akin to Merton (1976) where all jump risks are unpriced. If $\boldsymbol{\gamma} \neq 0$ and/or $\beta_i \neq 0$, changes occur in both jump-arrival intensities and jump-size distributions. Subsequently, in the empirical analysis attention is directed toward these parameters in the calibration process to establish the market risk premium for the defined risk classes, underscoring their pivotal role in the model.

For the derivation of a closed-form option pricing formula considering these factors, the money account is assumed as the numeraire (see, e.g., Geman et al., 1995). The resulting option price formula is based on the closed-form solution of Cheang and Chiarella (2011).[8] The dynamics of the asset prices under $\mathbb{Q}$ are expressed as:

$$\frac{X_i}{X_i} = rdt + \sigma_i d\tilde{W}i,t + \int_{\mathbb{R}} [\exp(y_i) - 1] q(dy, dt) + \int_{\mathbb{R}} [\exp(z_i) - 1] q(dz_i, dt) \qquad i \in \{1, 2\},$$

[8] Cheang and Chiarella (2011) defines the measure transformation using the Radon-Nikodym derivative, while this paper employs the Esscher transformation, more common in actuarial literature. The Radon-Nikodym derivative provides separate parameters for jump probability and size, whereas the Esscher transformation defines a measure $\mathbb{Q}$ with a single parameter. The procedure for deriving the closed-form solution remains unaffected by these different approaches. Furthermore, it can be shown that the parameters of the Radon-Nikodym derivative have a unique relation to the parameter dervied here.

where $\tilde{W}_{i,t}$ denotes standard Brownian motion components under $\mathbb{Q}$, and q represents the Poisson measures under $\mathbb{Q}$. Therefore, the option price for the exchange of the two assets can be formulated as:

$$
\begin{aligned}
C(S_1,S_2) = \sum_k \sum_m \sum_n \exp\big(-(\tilde{\lambda}_1+\tilde{\lambda}_2+\tilde{\lambda})(T-t)\big)\frac{(\tilde{\lambda}_1(T-t))^k}{k!}\frac{(\tilde{\lambda}_2(T-t))^m}{m!}\frac{(\tilde{\lambda}(T-t))^n}{n!} \\
\times\Bigg[S_1\exp\Big(-(\tilde{\lambda}_1\tilde{\kappa}_{Z_1}+\tilde{\lambda}\tilde{\kappa}_1)(T-t)+k\tilde{\alpha}_{11}+\frac{k\delta_{11}^2}{2}+n\tilde{\alpha}_1+\frac{n\delta_1^2}{2}\Big)\Phi(d_{1,t,k,m,n}) \\
-S_2\exp\Big(-(\tilde{\lambda}_2\tilde{\kappa}_{Z_2}+\tilde{\lambda}\tilde{\kappa}_2)(T-t)+m\tilde{\alpha}_{22}+\frac{m\delta_{22}^2}{2}+n\tilde{\alpha}_2+\frac{n\delta_2^2}{2}\Big)\Phi(d_{2,t,k,m,n})\Bigg]
\end{aligned}
$$

where:

$$
d_{1,t,k,m,n} = \frac{\ln(\frac{S_1}{S_2})+(-\tilde{\lambda}(\tilde{\kappa}_1-\tilde{\kappa}_2)-\tilde{\lambda}_1\tilde{\kappa}_{Z_1}+\tilde{\lambda}_2\tilde{\kappa}_{Z_2})(T-t)+\mu_{k,m,n}+\frac{\sigma_{k,m,n}^2(T-t)}{2}}{\sigma_{k,m,n}\sqrt{T-t}}
$$

$$
d_{2,t,k,m,n} = d_{1,t,k,m,n} - \sigma_{k,m,n}\sqrt{T-t},
$$

with:

$$
\mu_{k,m,n} = k(\tilde{\alpha}_{1,1}+\frac{\delta_{1,1}^2}{2}) - m(\tilde{\alpha}_{2,2}+\frac{\delta_{2,2}^2}{2}) + n(\tilde{\alpha}_1-\tilde{\alpha}_2+\frac{\delta^2}{2})
$$

$$
\sigma_{k,m,n}^2 = \sigma^2 + \frac{k\delta_{11}^2}{T-t} - \frac{m\delta_{22}^2}{T-t} + \frac{n\delta^2}{T-t},
$$

where:

$$
\delta^2 = \delta_1^2 + \delta_2^2 + \rho_Y\delta_1\delta_2.
$$

In the absence of jump risk, when $\tilde{\alpha}_i = \tilde{\alpha}_{ii} = 0$ and $\delta_i = \delta_{ii} = 0$, the jump intensity becomes zero, resulting in $\tilde{\kappa}_i = \tilde{\kappa}_{Z_i} = 0$ for $i \in \{1,2\}$. Consequently, the option pricing formula of Margrabe (1978) is received, returning to the original model utilized at the beginning of the section. Given that this paper examines a single-period model, the subsequent content adheres to the condition of $T-t=1$. This does not represent a limit but instead reflects non-life insurance contracts or catastrophe and cyber bonds, which are issued for a fixed term without adjustments during the period.

2.4 Alternative models and limits

To facilitate a comparison with the newly proposed option model OM, a standard model from expected value theory and an extension by Zanjani (2002) is presented. To maintain simplicity, no risk free discounting is applied. In standard model, the premium is defined as the expected loss plus frictional costs:

$$P = (1+\tau)\mathbb{E}[\bar{L}]. \tag{SM}$$

Zanjani (2002) introduce an extension to the standard model, focusing on the determination of (catastrophic) risk premiums. In his work, Zanjani highlights three primary considerations. Firstly, insurers may default due to heavy-tailed losses. Secondly, the cost associated with holding equity capital must be covered by premiums. Lastly, customers care about the insurer's risk of insolvency. According to Braun et al. (2023), the model can be summarized as follows:

$$P = \mathbb{E}[\bar{L}] - \mathbb{E}[D] + c. \tag{ZM}$$

Here, D denotes the difference between the expected payout and the realized payout in the event of insolvency:

$$D = max[\bar{L} - \bar{Y}_1, 0].$$

Since the default factor D also contains the premium, the model ZM does not have a closed-form solution. The cost of equity, denoted by c, is expressed as:

$$c = (\tau + r_{risk})S_0.$$

Here, r_{risk} signifies a risk premium determined by the correlation between loss and the capital market. This correlation is often assumed to be zero or close to zero for general insurance betas (e.g., Cummins and Harrington, 1985; Froot et al., 1995; Zanjani, 2002). Amidst the Covid-19 crisis, scholars have begun to recalibrate this term. Currently, there is no definitive evidence regarding the specific nature of this factor. It remains unclear whether it follows a linear pattern, e.g., Gründl et al. (2021), or exhibits concavity concerning the amount of risk, e.g., Braun et al. (2023). Furthermore, suitable models for parameter estimation have yet to be established. Therefore, either factor models or consumption-based approaches are used (e.g., Braun et al., 2019a; Braun et al., 2019b).

Both alternative pricing models rely on first-order terms. In contrast, the new OM model not only incorporates first-order terms but also identifies second-order terms as significant price drivers. Notably, terms related to the market environment are absent in the alternative models. While both models overlook market and loss uncertainties, the benchmark model also fails to consider any insolvency risks. Conversely, model ZM focuses solely on the insolvency risk for policyholders, without addressing the corresponding risk for shareholders.[9]

All pricing models should produce identical outcomes when jump risks, insolvency risks, and other frictions are removed. In such scenarios, the premium should correspond to the expected loss. This market is distinguished by either an infinite amount of equity or no variance.

[9] To adequately account for these factors, they would need to be encompassed within r_{risk} to prevent their neglect. However, this is not included in the definition of the factor.

Lemma 1. *Under the assumptions of a frictionless market without insolvency and jump risk, it is necessary for all models to satisfy:*

$$\lim_{S_0 \to \infty} P = \mathbb{E}[\bar{L}], \text{ and } \lim_{\sigma \to 0} P = \mathbb{E}[\bar{L}].$$

Proof. See Appendix A.3. □

With Lemma 1 established, the models exhibit convergence in a frictionless market without insolvency and jump risks. Additionally, OM model demonstrates its capability to incorporate non-linear insolvency risks and jump risks into pricing within market contexts.

Lemma 2. *In a frictionless market without insolvency risk but with a positive probability of jump occurrences, the influence of jump risk is negligible, and consequently, it remains unpriced. The premium equals the expected loss:*

$$\lim_{S_0 \to \infty} P = \mathbb{E}[\bar{L}].$$

Proof. See Appendix A.3. □

With model ZM as defined here, the insurability of correlated jump risks is not possible in an insolvency-free market context. In the presence of correlated jump risks where $r_{risk} > 0$, it follows that if S_0 tends towards infinity, P also tends towards infinity. This underlines the limits of a linear and constant factor approach when it comes to jump risks.

Despite the two alternative models presented here, there are also other possibilities. In the context of pricing cat bonds there are already contingent claim models that use compounded Poisson processes, such as models Lee and Yu (2002) or Ma and Ma (2013). However, the OM model presented here differs in three key aspects: First, it is applicable across all four risk classes, not just limited to cat bonds. Second, it provides a closed-form or straight-forward calculation, making it more practical and accessible. Third, it specifically prices the jump risk, rather than operating within the framework established by Merton (1976).

3 Premiums in the market

To validate the efficacy of the new OM model, its performance is demonstrated across all four risk categories and compared with existing models. This evaluation illustrates the model's enhanced capability in handling previously assessed risks. Subsequently, the model is applied to unique cyber risk data, showcasing that it can price risks that were not feasible with older approaches. The focus of this section is clearly on the cat and cyber bond market, the other risk categories complete the big picture of the wide range of applications. The demonstration underscores the OM model's broader applicability and improved performance in contemporary risk assessment.

3.1 Locally insurable risk

The shareholders' return is contingent upon the performance of the S&P 500 index. According to Morningstar (2023), the annual total return over the past decade has averaged approximately 9%, with a standard deviation of 15%. The assessment of locally insurable risk relies on U.S. indemnity losses, as documented in Frees and Valdez (1998). The dataset comprises 1,500 general liability claims, each representing indemnity payments in USD. For scaling purposes, the data is divided by 1,000, thus TUSD (thousands of USD) is used. This claims dataset is accessible through the R packages copula and evd. The expected loss per claim is 41.21 TUSD, with a standard deviation of 102.75 TUSD.

Figure 2 provides an overview of the premium relative to the expected loss for models SM, ZM and OM, (a) without frictions and (b) with frictions of $\tau = 0.05$. Since general insurance-related betas are close to zero, $r_{risk} = 0$ for the ZM model (Cummins and Harrington, 1985).

In the frictionless scenario, the premium of the SM model remains constant at 1. This outcome is anticipated, as insolvency risk and the market environment are not factored. Model ZM consistently exhibits the lowest premium since it only considers the insolvency risk for the policyholder, excluding risk for the shareholder. The OM model positions itself between the other two models. The latter two models reflect the expected framework: the lower the insolvency risk, the higher the risk premium, and they also demonstrate the in lemma 1 anticipated convergence towards the expected value. When frictions are included, the premium of the SM model increases but remains constant. The relationship between model ZM and OM also remains consistent. However, due to the frictions, both models no longer converge towards the expected value but instead increase exponentially. This exponential increase is attributed to the substantial equity required, as the frictions in the models are linear in equity, and the amount of equity needed to cover 1% of the tail does not grow linearly.

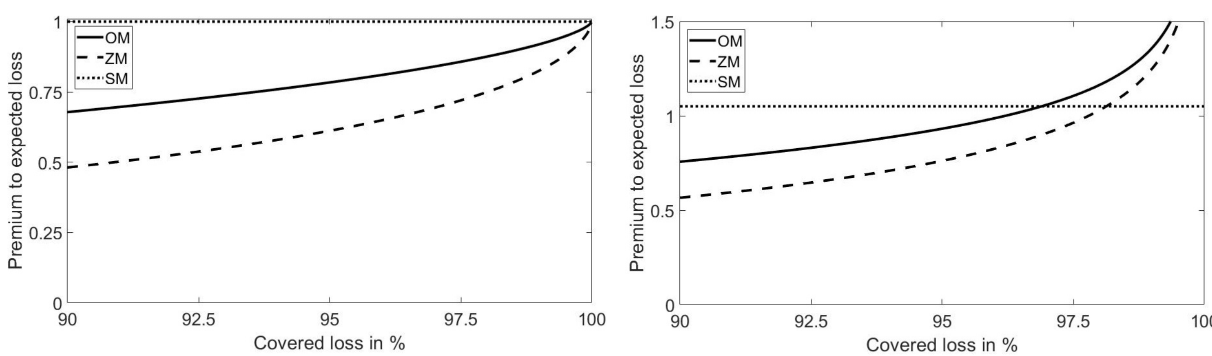

(a) Market with no frictons.

(b) Changing loss volatility.

Figure 1: Market with $\tau = 0.05$.

Figure 2: Premium for different models and market scenarios.

Figure 3 provides an overview of the risk premium for (a) various market volatilities and (b) different loss volatilities. The risk premium is calculated as the premium of model

OM minus the expected loss, adjusted for insolvency risk, using the truncated cumulative distribution function. As market volatility decreases, the risk premium increases because shareholders seek to invest their equity more securely, leading to higher premiums for policyholders seeking increased security. Conversely, when loss volatility increases, the risk premium also rises. Higher loss volatility implies greater uncertainty and insolvency risk for shareholders, who then demand a higher risk premium to compensate for the increased uncertainty.

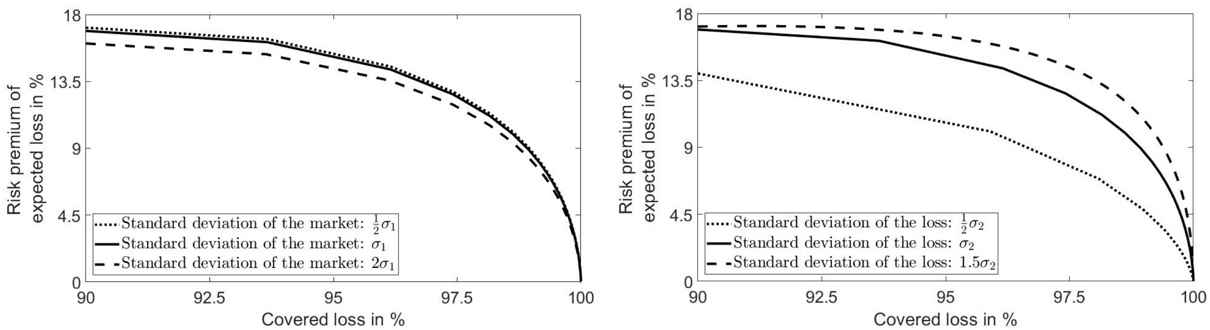

(a) Changing market volatility.

(b) Changing loss volatility.

Figure 3: Risk premium for different market and loss volatilities.

Hence, the model presented reflects the price dynamics for locally insurable risks that are prevalent in the insurance markets. Firstly, the assessment of payment default risk is of importance for policyholders. Secondly, the pricing mechanisms in the insurance markets are influenced in particular by insolvency risk and frictional costs. Thirdly, the risk premium is subject to the dynamic interplay of market volatility, loss uncertainty, and insolvency risk. Accordingly, the new OM model not only addresses jump risks, as will be demonstrated later, but also highlights the significance of incorporating higher orders to accurately reflect market conditions, for example, whether they are soft or hard.

3.2 Globally insurable risk

Data from Grinsted et al. (2019) encompasses the majority of United States hurricanes dating back to the early 20th century. In this section, extreme events are omitted, excluding the 10% of the most potent hurricanes (see Braun et al., 2023). Given the vulnerability of Texas and North Carolina to hurricanes and the absence of historical data indicating a hurricane simultaneously impacting both states (uncorrelated risk), these two states are used for the analysis. Following the data, Texas exhibits an expected annual hurricane loss of USD 1,685 million with a standard deviation 2.68 times the mean. North Carolina's expected annual hurricane loss amounts to USD 1,533 million with a standard deviation of 3.34 times the mean. The combined portfolio of hurricane losses for both states have an annual loss of USD 3,218 million with a standard deviation of 2.05 times the mean.

Two scenarios are used for comparison: one where the respective portfolios are insured locally, and another where a reinsurer covers the combined portfolio, thereby diversifying the associated risks. Figure 4 shows the equity needed for the respective (re)insurer to underwrite the risk. The reinsurer exhibits the highest capital requirement but concurrently manages the largest policy volume. When aggregating the capital requirements of local insurers, the reinsurer consistently demonstrates lower capital requirements for the same portfolio and same insolvency risk, where this effect becomes stronger with more tail risk. This phenomenon is due to the global diversification of reinsurance and underlines a fundamental aspect of reinsurance, namely the improved efficiency of risk diversification through an increased capital base. This observation is shown by Figure 5. By minimizing the portfolio variance, the reinsurer can charge a lower risk premium, which benefits the policyholder. However, this advantage diminishes if a hurricane affects both Texas and North Carolina, as the risk becomes correlated.

The SM model does not consider diversification (expected values are additive). The ZM model addresses this through the default variable D, as the default probability is influenced by the cumulative distribution function. Additionally, like the OM model, total frictional costs decrease with less equity.

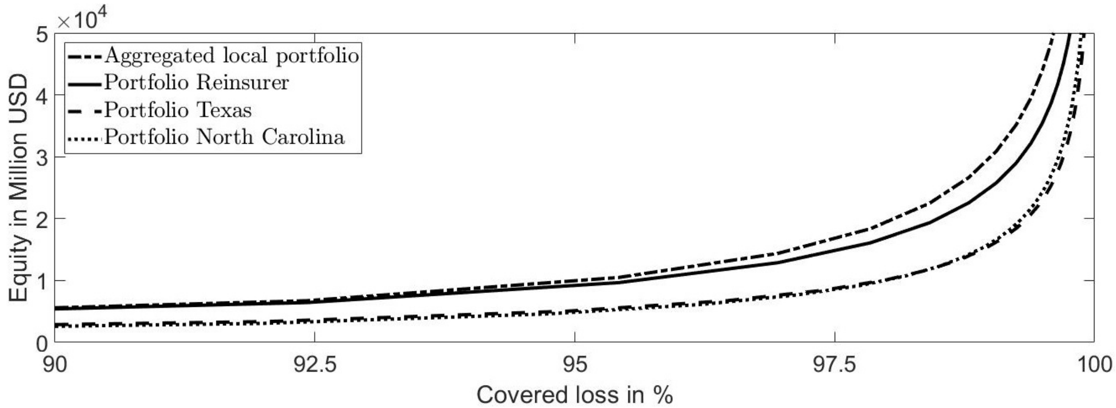

Figure 4: Equity for various local and global portfolios.

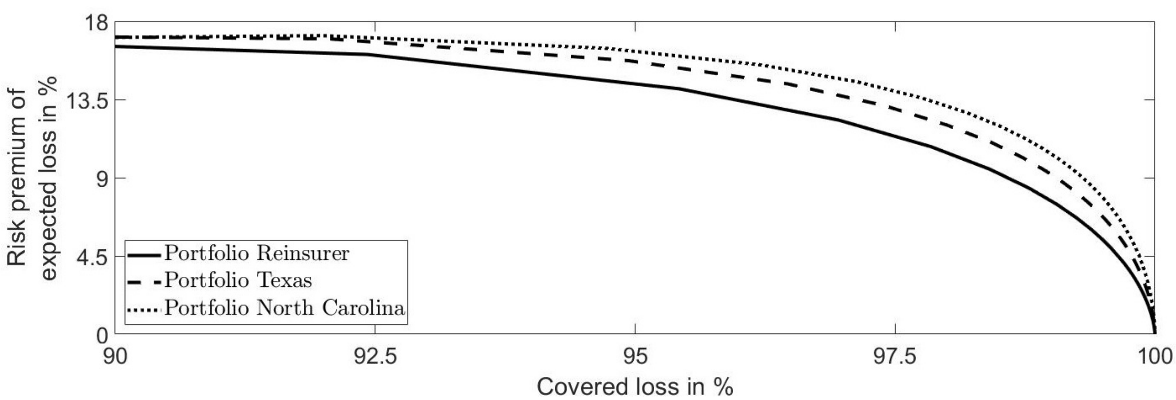

Figure 5: Risk premium for various local and global portfolios.

3.3 Globally diversifiable risk

Globally diversifiable risk refers to the type of risk that is primarily covered by the capital market due to the amount of capital required which cannot be adequately provided by (re)insurers alone. This transfer of risk to the capital market typically involves the issuance of a cat bond. Shareholders of the bond pay a principal amount N to a trust account at time $t = 0$. In return, at time $t = 1$, they receive the risk-free rate earned from the trust account, a coupon payment C, and the principal, and need to pay the incurred losses (and any additional expenses). Therefore, the terminal cash flow for the shareholder is given by:

$$\bar{Y}_1 = (1 + r_f)N + C,$$

whereby $\bar{H}_1$ and $\bar{T}_1$ remain the same. To ensure that the initial cash flow for shareholders remains consistent throughout the model, the initial cash flow is:

$$Y_0 = N = S_0 + \frac{C}{1+\omega}.$$

Here, ω represents a risk-adjusted discount rate, and $P = \frac{C}{1+\omega}$ denotes the present value premium paid by the policyholder (Braun et al., 2023).

Cat bonds typically have an attachment point beyond which they are activated. In this context, the trigger is set at the 90% quantile of annual hurricane losses, meaning that only losses exceeding USD 64,503 million are covered. Losses below this threshold remain within the insurance market or are borne by policyholders. Consequently, the insurance market anticipates an expected annual hurricane loss of USD 15,966 million, with a standard deviation approximately 1.32 times the mean. The cat bond is assumed to cover losses up to a maximum of USD 103,373 million, corresponding to the 95% quantile. If a hurricane triggers the cat bond, the expected loss, amounting to USD 26,949 million, falls into the capital market. This segment carries an expected annual hurricane loss with a standard deviation of around 0.53 times the expected value. The probability of such an event occurring is estimated at 10%. The hurricane data is retrieved from Grinsted et al. (2019).

The investment market is represented by the S&P 500, with the same assumptions as in the previous section. Based on historical market shocks from MFS (2023), it is assumed that a market crash occurs every 10 years with an average decline of 43.11% and a standard deviation of 0.34 times the expected value. Additionally, recent research found a frictional rate of 4.5% for cat bonds (Braun et al., 2023).

To compare Model OM with Model ZM, r_{risk} must be estimated. The latest estimate from Braun et al. (2023) is used, which employs the five-factor model from Fama and French (1993). Despite recent research to determine the factors for the risk premium of the cat bond market, there is still no widely accepted model (e.g., Braun et al., 2024). Firstly, data for cat bond indices has only been available for around 20 years, and secondly, it is difficult to represent the rare downside risks in a factor.

Three scenarios for the cat bond and the multiple of the bond, i.e., how many times the initial modeled expected loss investors receive in terms of the coupon, are examined (see Table 1). If the multiple equals 1, it indicates a coupon without a risk premium. A comparison with the SM model is unnecessary here, as it does not include any of the dynamics and would be constant at 1. In Scenario 1, the probability of the jump in loss is positive, the capital market has no jump risk, and there are no frictions. In this case, the multiple from model OM is approximately 1.07, indicating a market risk premium of 7% of the expected loss. If the capital market also has a risk of a crash, the market risk premium falls to around 2%. This is consistent with previous results showing that the more volatile the market, the lower the risk premium. Scenarios 1 and 2 are identical in the ZM model, as it does not include a market environment, and has a multiple of 1.0766. This proximity to Scenario 1 of the OM model is no coincidence and validates this model. The estimated jump risks have comparatively low volatility (small second order), there is no market environment taken into account, and the market and the risk are uncorrelated, which also underlines the comparatively small r_{risk}. Accordingly, it is to be expected that both models estimate a small risk premium. Since the ZM model cannot assess the market jump risk, it overestimates the risk premium at this point. In the last scenario, frictional costs are added, and the market risk premium rises to 58% for the OM model and to 76% for the ZM model. This aligns with previous research indicating that frictional costs account for a large part of the premium for extreme risks (e.g., Braun et al., 2019a; Braun et al., 2023). The higher risk premium of the ZM model can be explained by its linearity.

According to Artemis (2024b), the average multiple for the cat bond market for Q2 2024 is 4, meaning the risk premium is 300% of the expected loss. However, the market risk premium calculated here with the OM model is only around 57%. Assuming that the underlying cat bond is priced consistently with the market, a probability distortion can be assumed. As described in Gao et al. (2019), this distortion is a tail risk concern, which reflects investors' subjective ex-ante beliefs about tail risk. The parameters of the measure transformation must be calibrated accordingly.

In Scenario 4, the unique measure $\mathbb{Q}$ is calibrated. The ZM model alone cannot estimate a measure transformation. Accordingly, another model would first have to be used to determine the measure $\mathbb{Q}$. For comparability, the measure transformation estimated with the OM model is used here. The ZM model is unable to reflect the market price accurately due to its reliance on pure expected value structure, without accounting for jump risks and higher orders. In addition to the measure $\mathbb{Q}$, the estimation of the factor r_{risk} would also need to be different. However, this is challenging for linear factor models due to low correlations and rare downside risks. This reveals a disadvantage of the ZM model, which requires an additional factor or consumption-based model, 20 years of time series data, and a third model to measure $\mathbb{Q}$, whereas the OM model incorporates all these elements and does not require large time series data.

In the last scenario, Scenario 5, the frictional cost is removed for both models, for example through government support for the development of the cat bond market, under the measure $\mathbb{Q}$. A reduction in frictional costs can significantly reduce the risk premium, but it is still above the estimates with the $\mathbb{P}$ measure. Accordingly, the probability distortion of investors is another major cost driver, which was estimated here unique using the market calibration.

Scenario	Measure	Estimates OM	Estimates ZM	Cat bond multiple OM	Cat bond multiple ZM
1	$\mathbb{P}$	$\lambda_2 = 0.1$	$r_{risk} = 0.005$	1.0689	1.0766
2	$\mathbb{P}$	$\lambda_1 = \lambda_2 = 0.1$	$r_{risk} = 0.005$	1.0201	1.0766
3	$\mathbb{P}$	$\lambda_1 = \lambda_2 = 0.1$ $\tau = 0.045$	$r_{risk} = 0.005$ $\tau = 0.045$	1.5783	1.7622
4	$\mathbb{Q}$	$\lambda_1 = \lambda_2 = 0.1$ $\tau = 0.045$ $\beta_2 = -0.402$	$r_{risk} = 0.005$ $\tau = 0.045$	4	2.5557
5	$\mathbb{Q}$	$\lambda_1 = \lambda_2 = 0.1$ $\beta_2 = -0.402$	$r_{risk} = 0.005$	2.8781	1.1556

Table 1: Multiples for the cat bond without and with measure transformation, estimated with OM and ZM.

3.4 Globally undiversifiable risk

Based on the calibrations presented in the previous section, the pricing of a pandemic bond reveals that it is prohibitively expensive compared to other risk classes, making it difficult to transfer to the capital market without adjustments such as government support (e.g., Braun et al., 2023). It is important to note that, to date, no such instrument as a pandemic bond exists.

The analysis assumes a pandemic occurs twice per century, as evidenced by the Spanish flu and Covid-19 (Centers for Disease Control and Prevention, 2023). The S&P 500 serves as the underlying market, with the jump size derived from previous calibrations. Business interruptions, a component of property insurance contracts (APICA, 2020), are considered as losses caused by the pandemic, using the losses from the previous chapter as the baseline. To ensure comparability with cat bond, the same jump size is assumed. This involves adopting a lower limit for the jump process, recognizing that, in reality, undiversifiable jumps are significantly larger (e.g., APICA, 2020). Consequently, the jump probabilities are reduced, but the jump itself is included as a joint process with correlated jump sizes. A factor model approach to estimate r_{risk} is unsuitable due to the lack of a calibration market. Instead, a consumption-based approach can be utilized to capture the rare downside risk (e.g., Braun et al., 2019b). The most recent estimate from Braun et al. (2023), based on the Covid-19 pandemic, is used once again.

Table 2 displays the multiple for the pandemic bond. In Scenario 1, the joint jump is considered. Compared to the cat bond estimate, the multiple more than triples under the OM model, despite the probability of occurrence being only one-fifth. Due to the linear risk cost assumption of the ZM model and the high equity required, this model reaches a multiple of 16 under the $\mathbb{P}$ measure. Including frictional costs doubles the multiple for the OM model and increases it by approximately 20% for the ZM model. Although the tail risk, and therefore the ex-ante investor behavior, is likely to differ for pandemics than for natural disasters , due to limited data, it is assumed that the probability distortion is identical to the estimated cat bond distortion. Scenario 3 demonstrates that the resulting market risk premium is more than 16 times the expected loss. For comparison, the largest historical market multiple was 7.5 at the inception of cat bonds in 2001 (Artemis, 2024b). When considering the $\mathbb{Q}$ measure for the ZM, the multiple exceeds 43. This leads to the conclusion that, given the current market conditions, transferring pandemic risks through the capital market is not feasible (e.g., Gründl et al., 2021). Potential interventions could include reducing frictional costs; in Scenario 4, assuming no frictional costs, the multiple decreases to less than 11 for the OM and 35.5 for the ZM model. While a market risk premium of just under 1000% of the expected loss remains very high, it represents a significant reduction. However, it is important to note that a lower limit for the jump size was used here. If the jump size increases, the relative multiple may remain stable, but the absolute values become unaffordable. Additionally, the correlation of jump sizes was omitted. Since only extreme events with comparably low variance that occur together due to the Poisson process are considered, correlation has minimal impact on the multiple here. However, it is evident that linear models and previous asset pricing models, such as the consumption model, are unsuitable for measuring this type of extreme risk. As discussed in Braun et al. (2023), this risk should also follow a concave rather than a linear pattern.

In summary, the new pricing model reflects the essential relationships between risk and the market, a component missing in previous models. It can calculate market risk premiums based on the market environment, accommodating both hard and soft market conditions. Additionally, it can price jump risks, whether independent or joint, which is challenging for previous models due to the lack of suitable factor models and sufficient data to estimate the risk of heavy-tailed distributions. Furthermore, the OM model can measure an ex-ante investor attitude and thus calibrate a unique $\mathbb{Q}$ measure. With appropriate calibration, the market's risk appetite can be determined by entity and risk, as discussed in the next section. Beyond the scenarios considered here, many other combinations are conceivable. For instance, integrating market risk with jump risks into locally and globally insurable risks could further enhance the model's realism.

Scenario	Measure	Estimates OM	Estimates ZM	Pandemic bond multiple OM	Pandemic bond multiple ZM
1	$\mathbb{P}$	$\lambda = 0.02$	$r_{risk} = 0.206$	3.8122	16.1562
2	$\mathbb{P}$	$\lambda = 0.02$ $\tau = 0.045$	$r_{risk} = 0.206$ $\tau = 0.045$	6.6439	19.4670
3	$\mathbb{Q}$	$\lambda = 0.02$ $\tau = 0.045$ $\gamma_2 = -0.402$	$r_{risk} = 0.206$ $\tau = 0.045$	17.2916	43.1152
4	$\mathbb{Q}$	$\lambda = 0.02$ $\gamma_2 = -0.4026$	$r_{risk} = 0.206$	10.8625	35.5646

Table 2: Multiples for a fictive pandemic bond without and with measure transformation, estimated with OM and ZM.

3.5 Investors probability distortion

The next step in this analysis aims to understand the risk tolerance of specific market participants concerning natural catastrophe (NatCat) and cyber risks. For NatCat events, the calibration utilizes hurricane data from Grinsted et al. (2019). The analysis of cyber risk is based on a dataset obtained from a leading risk modeling agent and based on a loss portfolio from an global reinsurer, which represents the worldwide cyber risk market. Using this dataset, the risk modeling agent generated 10,000 losses, ranging from daily incidents to extreme events. Further details about the dataset are available in Kasper et al. (2024). To simplify the analysis, we assume there is no jump risk in the market and no frictions are present.

The goal is to assess the stability of the measure transformation in relation to individual market participants. While the previous chapter demonstrated how to calibrate a probability distortion based on market data, this section focuses on the sensitivity of this measure in the context of emerging risks, specifically NatCat and cyber risks. The analysis considers three market participants: (1) SwissRe, which issued a catastrophe bond and a cyber bond one year apart, (2) Chubb, and (3) Beazley, which has issued several cyber bonds with varying characteristics within a short timeframe. The study focuses on bonds for which a complete data set is available, as provided by Artemis (2024a) (see Table 3). Furthermore, the application of the new model and initial findings are presented here. A more in-depth analysis is part of the future research

Bond	Date of issue	Type	Cedent	Attachment point	Expected loss	Spread	Multiple
1	Jun 2022	US named storm	Swiss Re	3.82%	3.31%	9%	2.7190
2	Dec 2023	Cyber	Swiss Re	2.228%	1.721%	12%	6.9727
3	Dec 2023	Cyber	Chubb	2.142%	1.387%	9.25%	6.6691
4	Dec 2023	Cyber	Beazley	1.71%	1.26%	13%	10.3175

Table 3: Target bonds

Each bond is calibrated using the loss distributions and its specific properties. Table 4 presents the calibration results, including key metrics such as the proportional jump size, standard deviation, and the attachment and end quantiles of the bond. The final column lists the β_2 parameter, which defines the transformation specific to each bond. The distribution of the jumps and quantiles are calibrated based on the attachment point and the expected loss ratio, and the resulting β_2 based on the multiple and resulting in a unique transformation process.

Bond	Prop. jump size	std. dev. of the jump	Attachment quantile	End quantile	β_2
1	9.15	3.39	96.18%	99.06%	-0.2243
2	7.72	5.09	97.772%	99.617%	-0.7697
3	8.31	5.47	97.858%	99.697%	-0.7681
4	9.18	5.91	98.29%	99.699%	-0.9392

Table 4: Calibration output

The analysis indicates that each bond exhibits distinct characteristics in terms of jump sizes and coverage. For instance, NatCat bond (1) has a relatively large jump but a comparatively low standard deviation and tail coverage, resulting in the lowest concern for tail risk. Bonds (2) and (3), while slightly different, are most similar in their attachment points, expected losses, and multiples. Consequently, their calibrations show similar distributions and comparable probability distortions. This suggests that the measure $\mathbb{Q}$ may be less influenced by the cedent and instead uniquely reflects similar risks. Bond (4), which has the highest attachment point and covers the largest tail risk, shows the highest concern for tail risk.

In summary, the comparison of these four bonds demonstrates the varying levels of market participation and tail coverage for different risk types. It provides initial evidence that similar coverage of similar risks leads to a unique probability distortion that is independent of the cedent. Unlike the classic bond market, where the cedent significantly influences the spread, cat bonds and cyber bonds are fully covered and have no default risk. This finding suggests that the spread in this market primarily depends on the tail risk concerns of investors, leading to a homogeneous risk profile uniquely determined by $\mathbb{Q}$. Generally, it can be observed that higher tail coverage and standard deviation are associated with greater distortion, while jump size and attachment point have less influence. This analysis suggests that the OM model can be utilized not only for pricing but also for comparing market participants and assessing risk appetite, highlighting initial findings regarding the uniqueness of the risks covered.

3.6 Limitation and further research

A limitation of the OM model is its assumptions regarding distributions. In traditional insurance practices, it is often assumed that claims follow a lognormal distribution (e.g., Eling, 2012). However, the distribution of jump risks remains uncertain. Current approaches predominantly rely on expected value theory, assuming that Peaks over Threshold (POT) events follow a Generalized Pareto Distribution (GPD). The challenge is the lack of a universally accepted model for identifying POT events, the absence of an inherent upper limit to POT losses and the finite nature of the moments (McNeil et al., 2015). Insurance contracts and catastrophe bonds introduce constraints by imposing limits on payouts, necessitating the use of truncated distributions. For instance, Kasper et al. (2024) demonstrate that almost no "extreme tail" risk is covered in the cyber risk market. This raises the question of whether truncation favors the here chosen distributions as a potentially more suitable or at least acceptable choice (e.g., Ma and Ma, 2013), considering the model's other advantages, as similar processes are widely used for the catastrophic market (e.g., Lee and Yu, 2002; Jaimungal and Wang, 2006). This question presents an opportunity for future research. Furthermore, an option model can be developed that enhances reliance on extreme value theory and adjusts the distribution of jump risks within the GPD framework.

Another area for future research should focus on Section 3.5, examining more closely the uniqueness of $\mathbb{Q}$. This paper has already provided initial evidence that investors primarily define the spread based on tail risk concerns. However, since the primary focus here is on introducing the new model, this analysis should be expanded. In particular, a comparison between catastrophe bonds and cyber bonds could be made. This would require a similar data basis for NatCat events as for cyber events, possibly provided by a risk modeling agent, and more detailed information on the latest cyber bonds. Nevertheless, the model derived in this paper can be used for this comparison, as alternative models, such as those relying on time series data, are not applicable, e.g., due to the lack of time series data for cyber events.

4 Conclusion

This paper addresses the evolving landscape of risk management by proposing a novel model for pricing extreme risks, particularly in the context of insurance-linked securities such as catastrophe and cyber bonds. Given the increasing importance of jump risks and their correlation with macroeconomic fundamentals, particularly highlighted by events such as the Covid-19 pandemic, the need for more accurate pricing models is evident. The model presented in this paper not only updates existing risk categories but also integrates key market factors, correlation structures, and jump risks into a consistent framework. This approach deviates from traditional factor or consumption models, offering a more comprehensive understanding of risk premiums in the cat bond market. By incorporating real-world data and calibrating parameters accordingly, the paper provides a practical application of the model, demonstrating its effectiveness in pricing not only insurable risk but also cat bonds and cyber bonds. The findings suggest that the spread in these markets is primarily driven by investors' concerns about tail risk, as captured by the unique measure $\mathbb{Q}$, offering a more nuanced view than traditional models. This study contributes to the literature by providing a robust framework that accounts for higher-order risks and market frictions, paving the way for more precise risk assessment and management in the future.

References

Ai, H. and Bhandari, A. (2021). Asset pricing with endogenously uninsurable tail risk. *Econometrica*, 89(3):1471–1505.

Andersen, T. G., Fusari, N., and Todorov, V. (2020). The pricing of tail risk and the equity premium: Evidence from international option markets. *Journal of Business & Economic Statistics*, 38(3):662–678.

APICA (2020). APCIA Releases Update to Business Interruption Analysis.

Artemis (2024a). Catastrophe Bond & Insurance-Linked Securities Deal Directory. `https://www.artemis.bm/deal-directory`. [Online; accessed 25-July-2024.

Artemis (2024b). Catastrophe bonds and ILS average multiple by year. `https://www.artemis.bm/dashboard/cat_bonds_ils_average_multiple/`. [Online; accessed 09-February-2024].

Black, F. and Scholes, M. (1973). The pricing of options and corporate liabilities. *Journal of Political Economy*, 81(3):637–654.

Bollerslev, T. and Todorov, V. (2011). Tails, fears, and risk premia. *The Journal of Finance*, 66(6):2165–2211.

Bowers, N. L., Gerber, H. U., Hickman, J. C., Jones, D. A., and Nesbitt, C. (1986). *Actuarial Mathematics*. Itasca, Ill.: Society of Actuaries.

Braun, A., Ammar, S. B., and Eling, M. (2019a). Asset pricing and extreme event risk: Common factors in ils fund returns. *Journal of Banking & Finance*, 102:59–78.

Braun, A., Eling, M., and Freyschmidt, M. (2023). Optimal government intervention for extreme risks. *Available at SSRN*.

Braun, A., Herrmann, M., and Hibbeln, M. T. (2024). Common risk factors in the cross section of catastrophe bond returns. *Available at SSRN 3901695*.

Braun, A., Luca, D., and Schmeiser, H. (2019b). Consumption-based asset pricing in insurance markets: Yet another puzzle? *Journal of Risk and Insurance*, 86(3):629–661.

Caldana, R. and Fusai, G. (2013). A general closed-form spread option pricing formula. *Journal of Banking & Finance*, 37(12):4893–4906.

Centers for Disease Control and Prevention (2023). 100 years since 1918: Are we ready for the next pandemic?

Cheang, G. H. and Chiarella, C. (2011). Exchange options under jump-diffusion dynamics. *Applied Mathematical Finance*, 18(3):245–276.

Cummins, J. D. (2006). Should the government provide insurance for catastrophes? *Federal Reserve Bank of St. Louis Review*, 88(4):337–379.

Cummins, J. D. and Harrington, S. (1985). Property-liability insurance rate regulation: estimation of underwriting betas using quarterly profit data. *Journal of Risk and Insurance*, 52(1):16–43.

Cummins, J. D. and Phillips, R. D. (2005). Estimating the cost of equity capital for property-liability insurers. *Journal of Risk and Insurance*, 72(3):441–478.

Cummins, J. D. and Weiss, M. A. (2009). Convergence of insurance and financial markets: Hybrid and securitized risk-transfer solutions. *Journal of Risk and Insurance*, 76(3):493–545.

Dickerson, A., Mueller, P., and Robotti, C. (2023). Priced risk in corporate bonds. *Journal* *of Financial Economics*, 150(2):103707.

Doherty, N. A. and Garven, J. R. (1986). Price regulation in property-liability insurance: A contingent-claims approach. *Journal of Finance*, 41(5):1031–1050.

Eling, M. (2012). Fitting insurance claims to skewed distributions: Are the skew-normal and skew-student good models? *Insurance: Mathematics and Economics*, 51(2):239–248.

Esscher, F. (1932). On the probability function in the collective theory of risk. *Skandinavisk Aktuarietidskrift*, 15(3):175–195.

Fama, E. F. and French, K. R. (1993). Common risk factors in the returns on stocks and bonds. *Journal of Financial Economics*, 33(1):3–56.

Frees, E. W. and Valdez, E. A. (1998). Understanding relationships using copulas. *North American Actuarial Journal*, 2(1):1–25.

Froot, K. A., Murphy, B., Stern, A., and Usher, S. (1995). The emerging asset class: insurance risk. *Viewpoint*, 24(3). Originally "Special Report from Guy Carpenter and Company, Inc." July 1995.

Gao, G. P., Lu, X., and Song, Z. (2019). Tail risk concerns everywhere. *Management Science*, 65(7):3111–3130.

Geman, H., El Karoui, N., and Rochet, J.-C. (1995). Changes of numeraire, changes of probability measure and option pricing. *Journal of Applied Probability*, 32(2):443–458.

Gerber, H. U. and Shiu, E. S. (1994). Option pricing by esscher transforms. *Transactions of Society of Actuaries*, 46:99–191.

Grinsted, A., Ditlevsen, P., and Christensen, J. H. (2019). Normalized US hurricane damage estimates using area of total destruction, 1900-2018. *Proceedings of the National Academy of Sciences*, 116(48):23942–23946.

Gründl, H., Guxha, D., Kartasheva, A., and Schmeiser, H. (2021). Insurability of pandemic risks. *Journal of Risk and Insurance*, 88(4):863–902.

Harrison, J. M. and Pliska, S. R. (1981). Martingales and stochastic integrals in the theory of continuous trading. *Stochastic Processes and their Applications*, 11(3):215–260.

Jaimungal, S. and Wang, T. (2006). Catastrophe options with stochastic interest rates and compound poisson losses. *Insurance: Mathematics and Economics*, 38(3):469–483.

Kasper, D., Freyschmidt, M., Cremer, F., and Grossklags, J. (2024). Cyber risk: (Re)insurance meets capital markets. *Working Paper*.

Kelly, B. and Jiang, H. (2014). Tail risk and asset prices. *The Review of Financial Studies*, 27(10):2841–2871.

Lee, J.-P. and Yu, M.-T. (2002). Pricing default-risky cat bonds with moral hazard and basis risk. *Journal of Risk and Insurance*, pages 25–44.

Ma, Z.-G. and Ma, C.-Q. (2013). Pricing catastrophe risk bonds: A mixed approximation method. *Insurance: Mathematics and Economics*, 52(2):243–254.

Margrabe, W. (1978). The value of an option to exchange one asset for another. *Journal of Finance*, 33(1):177–186.

McNeil, A. J., Frey, R., and Embrechts, P. (2015). *Quantitative risk management: Concepts, techniques and tools-Revised edition*. Princeton university press.

Merton, R. C. (1976). Option pricing when underlying stock returns are discontinuous. *Journal of Financial Economics*, 3(1-2):125–144.

MFS (2023). Market Declines: A History of Recoveries.

Morningstar (2023). S&P 500. `https://www.morningstar.com/indexes/spi/spx/risk`. [Online; accessed 12-December-2023].

Ross, S. (2023). A History of the S&P 500 Dividend Yield. `https://www.investopedia.com/articles/markets/071616/history-sp-500-dividend-yield.asp`. [Online; accessed 01-February-2024].

Rubinstein, M. (1976). The valuation of uncertain income streams and the pricing of options. *The Bell Journal of Economics*, pages 407–425.

Runggaldier, W. J. (2003). Jump-diffusion models. In *Handbook of heavy tailed distributions in finance*, pages 169–209. Elsevier.

Wang, S. S. (2000). A class of distortion operators for pricing financial and insurance risks. *Journal of Risk and Insurance*, pages 15–36.

Zanjani, G. (2002). Pricing and capital allocation in catastrophe insurance. *Journal of Financial Economics*, 65(2):283–305.

A Appendix

A.1 Measure changes using the Esscher transformation

Define an asset as:

$$S_t = S_0 \exp(X_t),$$

where $X_t t \geq 0$ is a stochastic process characterized by stationary and independent increments, and $X_0 = 0$. Furthermore, let:

$$F_{X_t}(x) = \mathbb{P}(X_t \leq x)$$

be the cumulative distribution function, and:

$$M_{\mathbb{P},X_t}(u) = \mathbb{E}[\exp(uX_t)]$$

represent the moment-generating function of the random variable X_t under the measure $\mathbb{P}$. Thus:

$$M_{\mathbb{P},X_t}(u) = \int_{-\infty}^{\infty} \exp(ux) f(x,t) dx,$$

where $f(x,t)$ is the continuous density of X_t.[10] Building upon the transformation proposed by Esscher (1932), a transformed density for X_t is:

$$\begin{aligned} f(x,t,h) &= \frac{\exp(hx) f(x,t)}{\int_{-\infty}^{\infty} \exp(hy) f(y,t) dy} \\ &= \frac{\exp(hx) f(x,t)}{M_{\mathbb{P},X_t}(h)} \end{aligned}$$

where h is the transformation parameter. The corresponding moment-generating function is given by:

$$\begin{aligned} M_{Q,X_t}(u) &= \int_{-\infty}^{\infty} \exp(ux) f(x,t,h) dx \\ &= \frac{M_{\mathbb{P},X_t}(u+h)}{M_{\mathbb{P},X_t}(u)}. \end{aligned}$$

Subsequently, the Esscher transformation is derived for the three significant processes in this study. The analytical findings align with prior literature, exemplified by works such as Gerber and Shiu (1994) and Runggaldier (2003), where, for instance, Runggaldier transforms these measures utilizing the Radon-Nikodym theorem. In the provided examples, the time component is disregarded, as it is not needed in this context.

[10] For a discrete distribution, the integral can be replaced by a sum.

Normal distribution: Assuming $X_t = Y_t$, where Y_t is a normally distributed random variable with a mean of μ and a variance of σ^2. The moment-generating function is expressed as:

$$M_{\mathbb{P},X_t}(u) = \exp(u\mu + \frac{1}{2}\sigma^2 u^2).$$

Through the Esscher transformation, the resulting expression for the moment-generating function under the new measure $\mathbb{Q}$ is:

$$M_{\mathbb{Q},X_t}(u) = \exp\Big(u(\mu + h\sigma^2) + \frac{1}{2}\sigma^2 u^2\Big).$$

Consequently, the new mean under $\mathbb{Q}$ can be defined as $\tilde{\mu} = \mu + h\sigma^2$. The transformed normal distribution under $\mathbb{Q}$ remains a normal distribution with mean $\tilde{\mu}$ variance σ^2.

Proof.

$$\begin{aligned}\frac{M_{\mathbb{P},X_t}(u+h)}{M_{\mathbb{P},X_t}(u)} &= \frac{\exp\big((u+h)\mu + \frac{1}{2}\sigma^2(u+h)^2\big)}{\exp(u\mu + \frac{1}{2}\sigma^2 u^2)} \\ &= \exp\Big((u+h)\mu + \frac{1}{2}\sigma^2(u+h)^2 - (u\mu + \frac{1}{2}\sigma^2 u^2)\Big) \\ &= \exp\Big((h\mu + \frac{1}{2}\sigma^2 h^2 + \sigma^2 uh\Big) \\ &= \exp\Big((h(\mu + \sigma^2 u) + \frac{1}{2}\sigma^2 h^2\Big)\end{aligned}$$

□

Poisson distribution: Assume $X_t = kN_t$, where N_t is a Poisson process with intensity λ, and k is a constant. The moment-generating function is defined as:

$$M_{\mathbb{P},X_t}(u) = \exp\Big(\lambda(\exp(ku) - 1)\Big)$$

Through the Esscher transformation, the resulting expression for the moment-generating function under the new measure $\mathbb{Q}$ is:

$$M_{\mathbb{Q},X_t}(u) = \exp\Big(\lambda \exp(hk)(\exp(ku) - 1)\Big)$$

Consequently, the intensity under $\mathbb{Q}$ can be defined as $\tilde{\lambda} = \lambda \exp(hk)$. The transformed Poisson process under $\mathbb{Q}$ remains a Poisson process with intensity $\tilde{\lambda}$.

Proof.

$$\begin{aligned}\frac{M_{\mathbb{P},X_t}(u+h)}{M_{\mathbb{P},X_t}(u)} &= \frac{\exp\big(\lambda(\exp(k(u+h)) - 1)\big)}{\exp\big(\lambda(\exp(ku) - 1)\big)} \\ &= \exp\Big(\lambda(\exp(k(u+h)) - 1) - \lambda(\exp(ku) - 1)\Big) \\ &= \exp\Big(\lambda(\exp(ku)\exp(kh)) - \lambda\exp(ku)\Big) \\ &= \exp\Big(\lambda\exp(ku)(\exp(kh) - 1)\Big)\end{aligned}$$

□

Compounded Poisson process: Assume a compounded Poisson process $X_t = \sum_{i=1}^{N_t} Y_t$, where N_t is a Poisson process with intensity λ, and Y_t represents a normally distributed jump size with mean μ and variance σ^2. The moment-generating function is defined as:

$$\begin{aligned} M_{\mathbb{P},X_t}(u) &= \mathbb{E}[\exp(u\sum_{i=1}^{N_t} Y_i)] \\ &= \exp\big(\lambda(M_{\mathbb{P},Y_t}(u) - 1)\big) \end{aligned}$$

Through the Esscher transformation, the resulting expression for the moment-generating function under the new measure $\mathbb{Q}$ is:

$$M_{\mathbb{Q},X_t}(u) = \exp\Big(\lambda M_{\mathbb{P},Y_t}(h)(M_{\mathbb{Q},Y_t}(u) - 1)\Big)$$

Consequently, the intensity under $\mathbb{Q}$ can be defined as $\tilde{\lambda} = \lambda M_{\mathbb{P},Y_t}(h)$, and the new mean of the jump size under $\mathbb{Q}$ can be defined as $\tilde{\mu} = \mu + h\sigma^2$. The transformed compounded Poisson process under $\mathbb{Q}$ remains a compounded Poisson process with intensity $\tilde{\lambda}$ and mean jump size $\tilde{\mu}$ and variance σ^2.

Proof.

$$\begin{aligned} \frac{M_{\mathbb{P},X_t}(u+h)}{M_{\mathbb{P},X_t}(u)} &= \frac{\exp\big(\lambda(M_{\mathbb{P},Y_t}(u+h) - 1)\big)}{\exp\big(\lambda(M_{\mathbb{P},Y_t}(u) - 1)\big)} \\ &= \exp\Big(\lambda(M_{\mathbb{P},Y_t}(u+h) - 1) - \lambda(M_{\mathbb{P},Y_t}(u) - 1)\Big) \end{aligned}$$

Given the moment-generating function of a normally distributed random variable, one obtains:

$$\begin{aligned} M_{\mathbb{P},Y_t}(u+h) &= \exp\Big((u+h)\mu + \frac{1}{2}\sigma^2(u+h)^2\Big) \\ &= \exp\Big(u\mu + h\mu + \frac{1}{2}\sigma^2u^2 + \frac{1}{2}\sigma^2h^2 + \sigma^2uh\Big) \\ &= \exp\Big(u\mu + \frac{1}{2}\sigma^2u^2 + h(\mu + \sigma^2u) + \frac{1}{2}\sigma^2h^2\Big) \\ &= M_{\mathbb{P},Y_t}(u)M_{\mathbb{Q},Y_t}(h) \end{aligned}$$

Therefore:

$$\begin{aligned} \frac{M_{\mathbb{P},X_t}(u+h)}{M_{\mathbb{P},X_t}(u)} &= \exp\Big(\lambda(M_{\mathbb{P},Y_t}(u)M_{\mathbb{Q},Y_t}(h) - 1) - \lambda(M_{\mathbb{P},Y_t}(u) - 1)\Big) \\ &= \exp\Big(\lambda M_{\mathbb{P},Y_t}(u)M_{\mathbb{Q},Y_t}(h) - \lambda M_{\mathbb{P},Y_t}(u)\Big) \\ &= \exp\Big(\lambda M_{\mathbb{P},Y_t}(u)(M_{\mathbb{Q},Y_t}(h) - 1)\Big) \end{aligned}$$

□

A.2 Influence of dividends on premiums

Following Cheang and Chiarella (2011), both assets may yield a dividend return denoted as $\xi_i, i \in \{1,2\}$. In the context of this study, wherein S_2 represents the loss, dividend payments do not apply to this asset, resulting in $\xi_1 \geq 0$ and $\xi_2 = 0$. Consequently, the formulation of the option price for the exchange of the two assets, accounting for dividends, can be formulated as:

$$
\begin{aligned}
C(S_1, S_2) = &\sum_k \sum_m \sum_n \exp\big(-(\tilde{\lambda}_1 + \tilde{\lambda}_2 + \tilde{\lambda})\big) \frac{(\tilde{\lambda}_1)^k}{k!} \frac{(\tilde{\lambda}_2)^m}{m!} \frac{(\tilde{\lambda})^n}{n!} \\
&\times \Bigg[S_1 \exp\Big(-(\xi_1 + \tilde{\lambda}_1 \tilde{\kappa}_{Z_1} + \tilde{\lambda}\tilde{\kappa}_1) + k\tilde{\alpha}_{11} + \frac{k\delta_{11}^2}{2} + n\tilde{\alpha}_1 + \frac{n\delta_1^2}{2} \Big) \Phi(d_{1,t,k,m,n}) \\
&- S_2 \exp\Big(-(\tilde{\lambda}_2 \tilde{\kappa}_{Z_2} + \tilde{\lambda}\tilde{\kappa}_2) + m\tilde{\alpha}_{22} + \frac{m\delta_{22}^2}{2} + n\tilde{\alpha}_2 + \frac{n\delta_2^2}{2} \Big) \Phi(d_{2,t,k,m,n}) \Bigg]
\end{aligned}
$$

where:

$$
d_{1,t,k,m,n} = \frac{\ln(\frac{S_1}{S_2}) + (-\tilde{\lambda}(\tilde{\kappa}_1 - \tilde{\kappa}_2) - \tilde{\lambda}_1 \tilde{\kappa}_{Z_1} + \tilde{\lambda}_2 \tilde{\kappa}_{Z_2} - \xi_1) + \mu_{k,m,n} + \frac{\sigma_{k,m,n}^2}{2}}{\sigma_{k,m,n}\sqrt{T-t}}.
$$

The other terms remain unchanged.

Given the indemnity losses in the US from the example in Section 3.1. The dividend yield of the S&P 500 index was at the end of 2022 by 1.78%, whereas historical dividend yields for the S&P 500 index have typically ranged from between 3% to 5% (Ross, 2023). Figure 6 illustrates the premium differences between dividends and no dividends. The pattern resembles that seen with frictional costs. This suggests that dividends in alternative investments are a price determinant for insurance contract premiums.

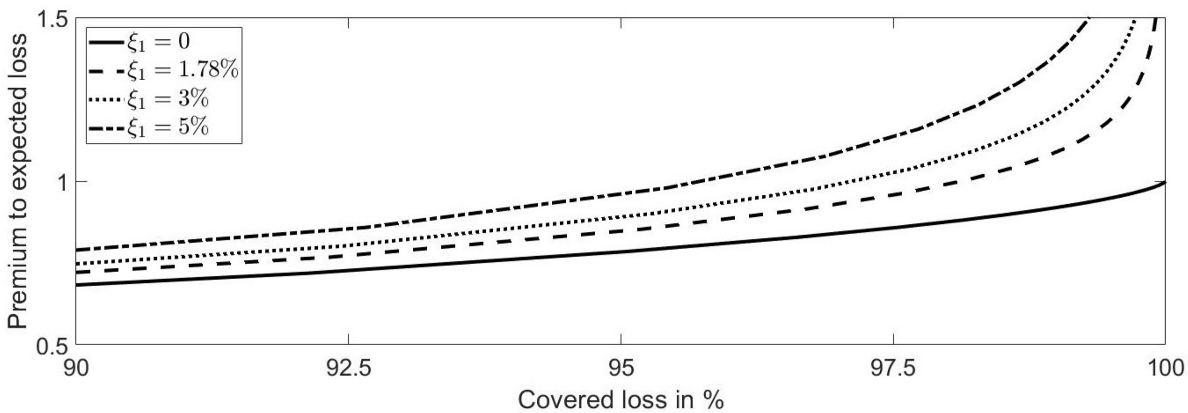

Figure 6: Premium for different dividends.

A.3 Proofs

Lemma 1

Proof. In the benchmark model, the proof is straightforward. In the extension, given the absence of insolvency risk, $E[D] = 0$. Moreover, without friction and jump risk, $c = 0$. Hence, $P = \mathbb{E}[\bar{L}]$. In the option model, when jump risk is absent, the following relationships hold:

$$
\begin{aligned}
& & Y_0\Phi(d_1) - \mathbb{E}[\bar{L}]\Phi(d_2) &= S_0 \\
\Leftrightarrow & & (S_0 + P)\Phi(d_1) - \mathbb{E}[\bar{L}]\Phi(d_2) &= S_0 \\
\Leftrightarrow & & S_0(\Phi(d_1) - 1) + P\Phi(d_1) - \mathbb{E}[\bar{L}]\Phi(d_2) &= 0
\end{aligned}
$$

It is observed that:

$$\lim_{S_0\to\infty} d_1 = \lim_{\sigma\to 0} d_1 = \infty \quad \text{and} \quad \lim_{S_0\to\infty} d_2 = \lim_{\sigma\to 0} d_2 = \infty,$$

leading to:

$$\lim_{S_0\to\infty} \Phi(d_1) = \lim_{\sigma\to 0} \Phi(d_1) = 1 \quad \text{and} \quad \lim_{S_0\to\infty} \Phi(d_2) = \lim_{\sigma\to 0} \Phi(d_2) = 1.$$

Consequently, the equation simplifies to:

$$
\begin{aligned}
& & S_0(\Phi(d_1) - 1) + P\Phi(d_1) - \mathbb{E}[\bar{L}]\Phi(d_2) &= 0 \\
\Leftrightarrow & & P - \mathbb{E}[\bar{L}] &= 0 \\
\Leftrightarrow & & P &= \mathbb{E}[\bar{L}]
\end{aligned}
$$

□

Lemma 2

Proof. In the scenario where $\sigma \to 0$, uncertainty diminishes, eliminating jump risks. Consequently, the focus lies solely on the case where $S_0 \to \infty$. Without loss of generality, k, m and n can be fixed:

$$
\begin{gathered}
\exp\big(-(\tilde{\lambda}_1 + \tilde{\lambda}_2 + \tilde{\lambda})\big)\frac{(\tilde{\lambda}_1)^k}{k!}\frac{(\tilde{\lambda}_2)^m}{m!}\frac{(\tilde{\lambda})^n}{n!} \\
= \\
\exp\big(-\tilde{\lambda}_1\big)\frac{(\tilde{\lambda}_1)^k}{k!}\exp\big(-\tilde{\lambda}_2\big)\frac{(\tilde{\lambda}_2)^m}{m!}\exp\big(-\tilde{\lambda}\big)\frac{(\tilde{\lambda})^n}{n!} \\
= \\
\mathbb{P}_{\tilde{\lambda}_1}(k)\mathbb{P}_{\tilde{\lambda}_2}(m)\mathbb{P}_{\tilde{\lambda}}(n),
\end{gathered}
$$

given the Poisson distribution of the jump occurrences. From the previous proof it is known that for $S_0 \to \infty$:

$$\Phi(d_1, t, k, m, n) = \Phi(d_2, t, k, m, n) = 1.$$

Thus, the option formula can be expressed as:

$$
\begin{aligned}
C(Y_1(P), \bar{L}) = &\sum_k \sum_m \sum_n \mathbb{P}_{\tilde{\lambda}_1}(k)\mathbb{P}_{\tilde{\lambda}_2}(m)\mathbb{P}_{\tilde{\lambda}}(n) \\
&\times \Bigg[Y_0 \exp\Big(-(\tilde{\lambda}_1\tilde{\kappa}_{Z_1} + \tilde{\lambda}\tilde{\kappa}_1) + k\tilde{\alpha}_{11} + \frac{k\delta_{11}^2}{2} + n\tilde{\alpha}_1 + \frac{n\delta_1^2}{2}\Big) \\
&- \mathbb{E}[\bar{L}] \exp\Big(-(\tilde{\lambda}_2\tilde{\kappa}_{Z_2} + \tilde{\lambda}\tilde{\kappa}_2) + m\tilde{\alpha}_{22} + \frac{m\delta_{22}^2}{2} + n\tilde{\alpha}_2 + \frac{n\delta_2^2}{2}\Big) \Bigg]
\end{aligned}
$$

Moreover:

$$
\begin{aligned}
\exp(k\tilde{\alpha}_{11} + \frac{k\delta_{11}^2}{2}) &= \mathbb{E}[\exp(kZ_1] \\
\exp(m\tilde{\alpha}_{22} + \frac{m\delta_{22}^2}{2}) &= \mathbb{E}[\exp(mZ_2)] \\
\exp(n\tilde{\alpha}_1 + \frac{n\delta_1^2}{2}) &= \mathbb{E}[\exp(nY_1)] \\
\exp(n\tilde{\alpha}_2 + \frac{n\delta_2^2}{2}) &= \mathbb{E}[\exp(nY_2)],
\end{aligned}
$$

and defining $\sum_{k,m,n} \mathbb{P}_{\tilde{\lambda}_1,\tilde{\lambda}_2,\tilde{\lambda}}(k,m,n) = \sum_k \sum_m \sum_n \mathbb{P}_{\tilde{\lambda}_1}(k)\mathbb{P}_{\tilde{\lambda}_2}(m)\mathbb{P}_{\tilde{\lambda}}(n)$:

$$
\begin{aligned}
C(Y_1(P), \bar{L}) = &\sum_{k,m,n} \mathbb{P}_{\tilde{\lambda}_1,\tilde{\lambda}_2,\tilde{\lambda}}(k,m,n) \Bigg[Y_0 \exp\Big(-(\tilde{\lambda}_1\tilde{\kappa}_{Z_1} + \tilde{\lambda}\tilde{\kappa}_1)\Big) \mathbb{E}[\exp(kZ_1)]\mathbb{E}[\exp(nY_1)] \\
&- \mathbb{E}[\bar{L}] \exp\Big(-(\tilde{\lambda}_2\tilde{\kappa}_{Z_2} + \tilde{\lambda}\tilde{\kappa}_2)\Big) \mathbb{E}[\exp(mZ_2)]\mathbb{E}[\exp(nY_2)] \Bigg] \\
= &\Bigg[Y_0 \exp\Big(-(\tilde{\lambda}_1\tilde{\kappa}_{Z_1} + \tilde{\lambda}\tilde{\kappa}_1)\Big) \sum_{k,m,n} \mathbb{P}_{\tilde{\lambda}_1,\tilde{\lambda}_2,\tilde{\lambda}}(k,m,n) \mathbb{E}[\exp(kZ_1)]\mathbb{E}[\exp(nY_1)] \\
&- \mathbb{E}[\bar{L}] \exp\Big(-(\tilde{\lambda}_2\tilde{\kappa}_{Z_2} + \tilde{\lambda}\tilde{\kappa}_2)\Big) \sum_{k,m,n} \mathbb{P}_{\tilde{\lambda}_1,\tilde{\lambda}_2,\tilde{\lambda}}(k,m,n) \mathbb{E}[\exp(mZ_2)]\mathbb{E}[\exp(nY_2)] \Bigg]
\end{aligned}
$$

The call option must equate to the initial equity, therefore:

$$
\begin{aligned}
C(Y_1(P), \bar{L}) = &(S_0 + P) \exp\Big(-(\tilde{\lambda}_1\tilde{\kappa}_{Z_1} + \tilde{\lambda}\tilde{\kappa}_1)\Big) \sum_{k,m,n} \mathbb{P}_{\tilde{\lambda}_1,\tilde{\lambda}_2,\tilde{\lambda}}(k,m,n) \mathbb{E}[\exp(kZ_1)]\mathbb{E}[\exp(nY_1)] \\
&- \mathbb{E}[\bar{L}] \exp\Big(-(\tilde{\lambda}_2\tilde{\kappa}_{Z_2} + \tilde{\lambda}\tilde{\kappa}_2)\Big) \sum_{k,m,n} \mathbb{P}_{\tilde{\lambda}_1,\tilde{\lambda}_2,\tilde{\lambda}}(k,m,n) \mathbb{E}[\exp(mZ_2)]\mathbb{E}[\exp(nY_2)] \\
= &S_0.
\end{aligned}
$$

For the sake of a simpler overview, let's define:

$$
J_1 = \sum_{k,m,n} \mathbb{P}_{\tilde{\lambda}_1,\tilde{\lambda}_2,\tilde{\lambda}}(k,m,n) \mathbb{E}[\exp(kZ_1)]\mathbb{E}[\exp(nY_1)]
$$

and:

$$J_2 = \sum_{k,m,n} \mathbb{P}_{\tilde{\lambda}_1,\tilde{\lambda}_2,\tilde{\lambda}}(k,m,n)\mathbb{E}[\exp(mZ_2)]\mathbb{E}[\exp(nY_2)]$$

as a placeholder. Isolating the premium yields to:

$$\begin{aligned}
P =&\mathbb{E}[\bar{L}]\frac{\exp\Big(-(\tilde{\lambda}_2\tilde{\kappa}_{Z_2}+\tilde{\lambda}\tilde{\kappa}_2)\Big)J_2}{\exp\Big(-(\tilde{\lambda}_1\tilde{\kappa}_{Z_1}+\tilde{\lambda}\tilde{\kappa}_1)\Big)J_1} + S_0\frac{1-\exp\Big(-(\tilde{\lambda}_1\tilde{\kappa}_{Z_1}+\tilde{\lambda}\tilde{\kappa}_1)\Big)J_1}{\exp\Big(-(\tilde{\lambda}_1\tilde{\kappa}_{Z_1}+\tilde{\lambda}\tilde{\kappa}_1)\Big)J_1} \\
=&\mathbb{E}[\bar{L}]\exp\Big(-(\tilde{\lambda}_2\tilde{\kappa}_{Z_2}-\tilde{\lambda}_1\tilde{\kappa}_{Z_1}+\tilde{\lambda}(\tilde{\kappa}_2-\tilde{\kappa}_1))\Big)\frac{J_2}{J_1} + S_0\frac{1-\exp\Big(-(\tilde{\lambda}_1\tilde{\kappa}_{Z_1}+\tilde{\lambda}\tilde{\kappa}_1)\Big)J_1}{\exp\Big(-(\tilde{\lambda}_1\tilde{\kappa}_{Z_1}+\tilde{\lambda}\tilde{\kappa}_1)\Big)J_1}
\end{aligned}$$

Upon closer examination of J_1, its expression can be rephrased. Without loss of generality, the same restructuring applies to J_2 by substituting k and m:

$$\begin{aligned}
J_1 &= \sum_{k,m,n} \mathbb{P}_{\tilde{\lambda}_1,\tilde{\lambda}_2,\tilde{\lambda}}(k,m,n)\mathbb{E}[\exp(kZ_1)]\mathbb{E}[\exp(nY_1)] \\
&= \underbrace{\sum_m \mathbb{P}_{\tilde{\lambda}_2}(m)}_{=1} \sum_k \mathbb{P}_{\tilde{\lambda}_1}(k)\mathbb{E}[\exp(kZ_1)] \sum_n \mathbb{P}_{\tilde{\lambda}}(n)\mathbb{E}[\exp(nY_1)].
\end{aligned}$$

Without loss of generality, the focus remains on $\sum_k \mathbb{P}_{\tilde{\lambda}_1}(k)\mathbb{E}[\exp(kZ_1)]$ with this equivalence extending to other components sharing a similar structure:

$$\begin{aligned}
\sum_k \mathbb{P}_{\tilde{\lambda}_1}(k)\mathbb{E}[\exp(kZ_1)] &= \sum_k \mathbb{P}_{\tilde{\lambda}_1}(k)\exp(k\tilde{\alpha}_{11} + k\frac{\delta_{22}^2}{2}) \\
&= \sum_k \mathbb{P}_{\tilde{\lambda}_1}(k)\exp(\tilde{\alpha}_{11} + \frac{\delta_{22}^2}{2})^k \\
&= \sum_k \mathbb{P}_{\tilde{\lambda}_1}(k)\mathbb{E}[\exp(Z_1)]^k \\
&= \sum_k \mathbb{P}_{\tilde{\lambda}_1}(k)\exp\big(k\ln(\mathbb{E}[\exp(Z_1)])\big)
\end{aligned}$$

Reflecting on the fact that the moment-generating function of a Poisson-distributed random variable x is defined as $M_X(u) = \mathbb{E}[\exp(uX)] = \sum_n \mathbb{P}(X=n)\exp(un)$, this results in:

$$\begin{aligned}
\sum_k \mathbb{P}_{\tilde{\lambda}_1}(k)\exp\big(k\ln(\mathbb{E}[\exp(Z_1)])\big) &= M_{N_1}\big(ln(M_{Z_1})\big) \\
&= \exp(\tilde{\lambda}_1(\exp\big(\ln(\mathbb{E}[\exp(Z_1)])\big)-1)) \\
&= \exp(\tilde{\lambda}_1\underbrace{\big(\mathbb{E}[\exp(Z_1)]-1)}_{\tilde{\kappa}_{Z1}}\big) \\
&= \exp(\tilde{\lambda}_1\tilde{\kappa}_{Z1}).
\end{aligned}$$

Summarized, it holds:

$$J_1 = \exp(\tilde{\lambda}_1 \tilde{\kappa}_{Z1}) \exp(\tilde{\lambda}\tilde{\kappa}_1)$$
$$J_2 = \exp(\tilde{\lambda}_2 \tilde{\kappa}_{Z2}) \exp(\tilde{\lambda}\tilde{\kappa}_2)$$

Therefore, the following applies to the premium:

$$\begin{aligned}
P =&\mathbb{E}[\bar{L}] \exp\Big(-(\tilde{\lambda}_2\tilde{\kappa}_{Z_2} - \tilde{\lambda}_1\tilde{\kappa}_{Z_1} + \tilde{\lambda}(\tilde{\kappa}_2 - \tilde{\kappa}_1))\Big) \frac{\exp(\tilde{\lambda}_2\tilde{\kappa}_{Z2}) \exp(\tilde{\lambda}\tilde{\kappa}_2)}{\exp(\tilde{\lambda}_1\tilde{\kappa}_{Z1}) \exp(\tilde{\lambda}\tilde{\kappa}_1)} \\
&+ S_0 \frac{1 - \exp\Big(-(\tilde{\lambda}_1\tilde{\kappa}_{Z_1} + \tilde{\lambda}\tilde{\kappa}_1)\Big) \exp(\tilde{\lambda}_1\tilde{\kappa}_{Z1}) \exp(\tilde{\lambda}\tilde{\kappa}_1)}{\exp\Big(-(\tilde{\lambda}_1\tilde{\kappa}_{Z_1} + \tilde{\lambda}\tilde{\kappa}_1)\Big) \exp(\tilde{\lambda}_1\tilde{\kappa}_{Z1}) \exp(\tilde{\lambda}\tilde{\kappa}_1)} \\
=&\mathbb{E}[\bar{L}] \exp\Big(-(\tilde{\lambda}_2\tilde{\kappa}_{Z_2} - \tilde{\lambda}_1\tilde{\kappa}_{Z_1} + \tilde{\lambda}(\tilde{\kappa}_2 - \tilde{\kappa}_1))\Big) \exp\Big((\tilde{\lambda}_2\tilde{\kappa}_{Z_2} - \tilde{\lambda}_1\tilde{\kappa}_{Z_1} + \tilde{\lambda}(\tilde{\kappa}_2 - \tilde{\kappa}_1))\Big) \\
&+ S_0 \frac{1 - \exp\Big(-(\tilde{\lambda}_1\tilde{\kappa}_{Z_1} + \tilde{\lambda}\tilde{\kappa}_1)\Big) \exp(\tilde{\lambda}_1\tilde{\kappa}_{Z1} + \tilde{\lambda}\tilde{\kappa}_1)}{\exp\Big(-(\tilde{\lambda}_1\tilde{\kappa}_{Z_1} + \tilde{\lambda}\tilde{\kappa}_1)\Big) \exp(\tilde{\lambda}_1\tilde{\kappa}_{Z1} + \tilde{\lambda}\tilde{\kappa}_1)} \\
&= \mathbb{E}[\bar{L}]
\end{aligned}$$

□